

The Study of the contribution of the LHT model to $Zb\bar{b}$ coupling

Bingfang Yang^{1,2}, Xuelei Wang¹, and Jinzhong Han¹

¹ *College of Physics and Information Engineering,
Henan Normal University, Xinxiang 453007, China*

² *Basic Teaching Department, Jiaozuo University, Jiaozuo 454000, China*

Abstract

In the framework of the Littlest Higgs Model with T-parity (LHT), we study the contributions of the new particles to $Zb\bar{b}$ couplings at one-loop level. Based on these results, we further study the branching ratio R_b and the unpolarized forward-backward asymmetry A_{FB}^b . We find that the correction of the new particles to $Zb\bar{b}$ couplings is mainly on the left-handed coupling and has small part of the parameter space to alleviate the deviation between theoretical predictions and experimental values. The precision measurement value of R_b can give severe constraints on the relevant parameters. The constraints from the precision measurement value of A_{FB}^b are very weak.

PACS numbers: 14.65.Fy, 12.60.-i, 12.15.Mm, 13.85.Lg

I. INTRODUCTION

The Standard Model (SM) has been very successful, however, it is still believed to be a theory effective at the electroweak scale and some new physics (NP) must exist at higher energy regimes. So far there have been many speculations on the possible forms of the NP beyond the SM, one of the interesting possibilities is the Little Higgs model. The little Higgs theory was proposed [1] as a possible solution to the hierarchy problem and remains a popular candidate for the NP. The Littlest Higgs (LH) model [2] is a cute economical implementation of the little Higgs, but suffered from severe constraints from electroweak precision tests [3], which would require raising the mass scale of the new particles to far above TeV scale and thus reintroduce the fine-tuning in the Higgs potential [4]. The most serious constraints resulted from the tree-level corrections to precision electroweak observables due to the exchanges of the additional heavy gauge bosons present in the theories, as well as from the small but non-vanishing vacuum expectation value (VEV) of an additional weak-triplet scalar field. In order to solve this problem, a discrete symmetry called T-parity is proposed [5], which explicitly forbids any tree-level contributions from the heavy gauge bosons to the observables involving only the SM particles as external states. The interactions that induce triplet VEV contributions is also forbidden. This model is called the Littlest Higgs Model with T-parity (LHT). In the LHT model, corrections to the precision electroweak observables are generated exclusively at loop level.

The branching ratio R_b is very sensitive to the NP beyond the SM, the precision experimental value of R_b may give a severe constraint on the NP [6]. Experimentally, the electroweak observables have been precisely measured at the SLC and LEP, in the most recent analysis of the electroweak data, $R_b = 0.21629 \pm 0.00066$ differs from the SM fit by 0.7σ , $A_{FB}^b = 0.0992 \pm 0.0016$ disagrees with the SM fit by -2.9σ [7]. Furthermore, the experimental value of $Zb\bar{b}$ couplings disagrees with the SM fit by about 3σ , especially the deviation of the right-handed coupling is so large that it is very difficult to explain. These significant deviations from the A_{FB}^b and the $Zb\bar{b}$ couplings might be the first window into the NP. With the running of the LHC, they will be further researched. In the LHT model, there are new fermions and new gauge bosons, which can contribute to the $Zb\bar{b}$ couplings and give modifications to the R_b and A_{FB}^b . Therefore, it is possible to give some constraints on the relevant parameters via their radiative corrections to the R_b and A_{FB}^b .

In this paper, we calculate the contributions of the LHT model to the $Zb\bar{b}$ couplings. On this basis, we further study the R_b and A_{FB}^b , then we give the constraints on the relevant parameters according to the precision measurements.

This paper is organized as follows. In Sec.II we recapitulate the LHT model and discuss the new flavor interactions which will contribute to the $Zb\bar{b}$ vertex. In Sec.III we calculate the one-loop contributions of the LHT model to the $Zb\bar{b}$ vertex, R_b and A_{FB}^b , then the relevant numerical results are shown. Finally, we give our conclusions in Sec.IV.

II. A BRIEF REVIEW OF THE LHT MODEL

The LHT [5] is based on a non-linear sigma model describing the spontaneous breaking of a global $SU(5)$ down to a global $SO(5)$. This symmetry breaking takes place at the scale $f \sim \mathcal{O}(TeV)$ and originates from the VEV of an $SU(5)$ symmetric tensor Σ , given by

$$\Sigma_0 \equiv \langle \Sigma \rangle = \begin{pmatrix} 0_{2 \times 2} & 0 & 1_{2 \times 2} \\ 0 & 1 & 0 \\ 1_{2 \times 2} & 0 & 0_{2 \times 2} \end{pmatrix} \quad (1)$$

From the $SU(5)/SO(5)$ breaking, there arise 14 Goldstone bosons which are described by the ‘‘pion’’ matrix Π , given explicitly by

$$\Pi = \begin{pmatrix} -\frac{\omega^0}{2} - \frac{\eta}{\sqrt{20}} & -\frac{\omega^+}{\sqrt{2}} & -i\frac{\pi^+}{\sqrt{2}} & -i\phi^{++} & -i\frac{\phi^+}{\sqrt{2}} \\ -\frac{\omega^-}{\sqrt{2}} & \frac{\omega^0}{2} - \frac{\eta}{\sqrt{20}} & \frac{v+h+i\pi^0}{2} & -i\frac{\phi^+}{\sqrt{2}} & \frac{-i\phi^0+\phi^P}{\sqrt{2}} \\ i\frac{\pi^-}{\sqrt{2}} & \frac{v+h-i\pi^0}{2} & \sqrt{4/5}\eta & -i\frac{\pi^+}{\sqrt{2}} & \frac{v+h+i\pi^0}{2} \\ i\phi^{--} & i\frac{\phi^-}{\sqrt{2}} & i\frac{\pi^-}{\sqrt{2}} & -\frac{\omega^0}{2} - \frac{\eta}{\sqrt{20}} & -\frac{\omega^-}{\sqrt{2}} \\ i\frac{\phi^-}{\sqrt{2}} & \frac{i\phi^0+\phi^P}{\sqrt{2}} & \frac{v+h-i\pi^0}{2} & -\frac{\omega^+}{\sqrt{2}} & \frac{\omega^0}{2} - \frac{\eta}{\sqrt{20}} \end{pmatrix} \quad (2)$$

Under T-parity the SM Higgs doublet, $H = (-i\pi^+\sqrt{2}, (v+h+i\pi^0)/2)^T$ is T-even while other fields are T-odd.

The Goldstone bosons $\omega^\pm, \omega^0, \eta$ are respectively eaten by the new T-odd gauge bosons W_H^\pm, Z_H, A_H , which obtain masses at $\mathcal{O}(v^2/f^2)$

$$M_{W_H} = M_{Z_H} = gf(1 - \frac{v^2}{8f^2}), M_{A_H} = \frac{g'f}{\sqrt{5}}(1 - \frac{5v^2}{8f^2}) \quad (3)$$

with g and g' being the SM $SU(2)$ and $U(1)$ gauge couplings, respectively.

The Goldstone bosons π^\pm, π^0 are eaten by the T-even W_L^\pm and Z_L bosons of the SM, which obtain masses at $\mathcal{O}(v^2/f^2)$

$$M_{W_L} = \frac{gv}{2}(1 - \frac{v^2}{12f^2}), M_{Z_L} = \frac{gv}{2\cos\theta_W}(1 - \frac{v^2}{12f^2}) \quad (4)$$

The photon A_L is also T-even and remains massless.

For each SM fermion, a copy of mirror fermion with T-odd quantum number is added in order to preserve the T-parity. For the mirror quarks, we denote them by u_H^i, d_H^i , where $i = 1, 2, 3$ are the generation index. At the order of $\mathcal{O}(v^2/f^2)$ their masses are given by

$$m_{d_H^i} = \sqrt{2}\kappa_i f, m_{u_H^i} = m_{d_H^i}(1 - \frac{v^2}{8f^2}) \quad (5)$$

where κ_i are the diagonalized Yukawa couplings of the mirror quarks.

In order to cancel the quadratic divergence of the Higgs mass induced by top loops, an additional heavy quark T^+ is introduced, which is even under T-parity. The implementation of T-parity then requires also a T-odd partner T^- . Their masses are given by

$$m_{T^+} = \frac{f}{v} \frac{m_t}{\sqrt{x_L(1-x_L)}} [1 + \frac{v^2}{f^2} (\frac{1}{3} - x_L(1-x_L))] \quad (6)$$

$$m_{T^-} = \frac{f}{v} \frac{m_t}{\sqrt{x_L}} [1 + \frac{v^2}{f^2} (\frac{1}{3} - \frac{1}{2}x_L(1-x_L))] \quad (7)$$

where x_L is the mixing parameter between the SM top-quark t and the new top-quark T^+ .

Just like the SM, the mirror sector in the LHT model also has weak mixing, parameterised by unitary mixing matrices: two for mirror quarks and two for mirror leptons:

$$V_{Hu}, V_{Hd}, V_{Hl}, V_{H\nu} \quad (8)$$

V_{Hu} and V_{Hd} are for the mirror quarks which are present in our analysis. V_{Hu} and V_{Hd} satisfy the physical constraints $V_{Hu}^\dagger V_{Hd} = V_{CKM}$. We follow [8] to parameterize V_{Hd} with three angles $\theta_{12}^d, \theta_{23}^d, \theta_{13}^d$ and three phases $\delta_{12}^d, \delta_{23}^d, \delta_{13}^d$

$$V_{Hd} = \begin{pmatrix} c_{12}^d c_{13}^d & s_{12}^d c_{13}^d e^{-i\delta_{12}^d} & s_{13}^d e^{-i\delta_{13}^d} \\ -s_{12}^d c_{23}^d e^{i\delta_{12}^d} - c_{12}^d s_{23}^d s_{13}^d e^{i(\delta_{13}^d - \delta_{23}^d)} & c_{12}^d c_{23}^d - s_{12}^d s_{23}^d s_{13}^d e^{i(\delta_{13}^d - \delta_{12}^d - \delta_{23}^d)} & s_{23}^d c_{13}^d e^{-i\delta_{23}^d} \\ s_{12}^d s_{23}^d e^{i(\delta_{12}^d + \delta_{23}^d)} - c_{12}^d c_{23}^d s_{13}^d e^{i\delta_{13}^d} & -c_{12}^d s_{23}^d e^{i\delta_{23}^d} - s_{12}^d c_{23}^d s_{13}^d e^{i(\delta_{13}^d - \delta_{12}^d)} & c_{23}^d c_{13}^d \end{pmatrix} \quad (9)$$

III. THE ONE-LOOP CORRECTIONS TO $Zb\bar{b}$ COUPLINGS IN THE LHT MODEL

We employ the following notation for the effective $Zb\bar{b}$ interaction:

$$\begin{aligned} L_{Zb\bar{b}} &= \frac{e}{S_W C_W} (g_L^b \bar{b} \gamma^\mu b P_L + g_R^b \bar{b} \gamma^\mu b P_R) Z_\mu \\ &= \frac{e}{2S_W C_W} \bar{b} \gamma^\mu (g_V^b - g_A^b \gamma_5) b Z_\mu \end{aligned} \quad (10)$$

where θ_W is the Weinberg angle, $S_W = \sin \theta_W$, $C_W = \cos \theta_W$, $P_L = \frac{1-\gamma_5}{2}$ and $P_R = \frac{1+\gamma_5}{2}$.

The effective couplings are then written as

$$\bar{g}_{L,R}^b = g_{L,R}^b + \delta g_{L,R}^{SM} + \delta g_{L,R}^{NP} \quad (11)$$

$$\bar{g}_{V,A}^b = g_{V,A}^b + \delta g_{V,A}^{SM} + \delta g_{V,A}^{NP} \quad (12)$$

where $\bar{g}_{L,R}^b, \bar{g}_{V,A}^b$ are respectively the radiatively-corrected effective couplings, $g_{L,R}^b$ are respectively the left-handed and right-handed $Zb\bar{b}$ couplings at tree level, $\delta g_{L,R}^{SM}$ and $\delta g_{L,R}^{NP}$ are their corresponding one-loop corrections of the SM and the NP, $g_{V,A}^b$ are respectively the vector and axial vector coupling coefficients of $Zb\bar{b}$ interaction at tree level, $\delta g_{V,A}^{SM}$ and $\delta g_{V,A}^{NP}$ are their corresponding one-loop corrections of the SM and the NP. The tree-level couplings are given by

$$g_L^b = -\frac{1}{2} + \frac{1}{3} S_W^2 \quad , \quad g_R^b = \frac{1}{3} S_W^2 \quad (13)$$

$$g_V^b = g_L^b + g_R^b = -\frac{1}{2} + \frac{2}{3} S_W^2 \quad , \quad g_A^b = g_L^b - g_R^b = -\frac{1}{2} \quad (14)$$

The branching ratio is defined as

$$R_b = \frac{\Gamma(Z \rightarrow b\bar{b})}{\Gamma(Z \rightarrow \text{hadrons})} \quad (15)$$

The full hadron width is the sum of widths of five quark channels:

$$\Gamma(Z \rightarrow \text{hadrons}) = \Gamma(Z \rightarrow u\bar{u}) + \Gamma(Z \rightarrow d\bar{d}) + \Gamma(Z \rightarrow s\bar{s}) + \Gamma(Z \rightarrow c\bar{c}) + \Gamma(Z \rightarrow b\bar{b}) \quad (16)$$

For the decays to any of the five pairs of quarks $q\bar{q}$ we have[9]

$$\Gamma_q \equiv \Gamma(Z \rightarrow q\bar{q}) = 12\Gamma_0 (g_{Aq}^2 R_{Aq} + g_{Vq}^2 R_{Vq}) \quad (17)$$

with $\Gamma_0 = \frac{G_F M_{Z_L}^3}{24\sqrt{2}\pi}$, here g_{Aq} and g_{Vq} are the axial-vector and effective vector couplings. The radiators R_{Aq} and R_{Vq} contain contributions from the final state gluons and photons. In the crudest approximation

$$R_{Vq} = R_{Aq} = 1 + \frac{\hat{\alpha}_s}{\pi} \quad (18)$$

where $\alpha_s(q^2)$ is the QCD running coupling constant:

$$\hat{\alpha}_s \equiv \alpha_s(q^2 = M_{Z_L}^2) \quad (19)$$

The expression of the radiative correction to R_b can be expressed as [10]

$$\delta R_b \simeq \frac{2R_b^{SM}(1 - R_b^{SM})}{g_{Vb}^2(3 - \beta^2) + 2g_{Ab}^2\beta^2} [g_{Vb}(3 - \beta^2)\delta g_{Vb} + 2g_{Ab}\beta^2\delta g_{Ab}] \quad (20)$$

with $\beta = \sqrt{1 - \frac{4\hat{m}_b^2}{M_{Z_L}^2}}$ being the velocity of b-quark in Z decay, here \hat{m}_b is the value of the running mass of the b-quark at scale M_{Z_L} calculated in \overline{MS} scheme [11].

The unpolarized forward-backward asymmetry in the decay to $b\bar{b}$ equals:

$$A_{FB}^b = \frac{N_F - N_B}{N_F + N_B} \quad (21)$$

where N_F is the cross section for finding the scattered fermion in the hemisphere defined by the incident electron direction and N_B is the cross section for finding it in the positron hemisphere. It can be expressed as

$$A_{FB}^b = \frac{3}{4} \left(1 - \frac{k_A}{\pi}\right) A_e A_b \quad (22)$$

where the factor $(1 - \frac{k_A}{\pi})$ represents a QCD radiative correction, as in Ref. [12], for which we use the numerical value 0.95, A_e refers to the creation of Z boson in e^+e^- -annihilation, while A_b is the left-right coupling constant asymmetry refers to its decay in $b\bar{b}$ [9]

$$A_b = \frac{2g_{Ab}g_{Vb}}{\beta^2 g_{Ab}^2 + (3 - \beta^2)g_{Vb}^2/2} \quad (23)$$

The relevant Feynman diagrams for the LHT contributions are shown in Fig.1. We use the 't Hooft-Feynman gauge, so the contributions of Goldstone bosons should be involved. In our calculation, g_{Ab} and g_{Vb} should be replaced by \bar{g}_{Ab} and \bar{g}_{Vb} , $g_{V,A}^b + \delta g_{V,A}^{SM}$ can be found in Ref. [13]. The calculations of the loop diagrams are straightforward. Each loop diagram is composed of some scalar loop functions [14], which are calculated by using

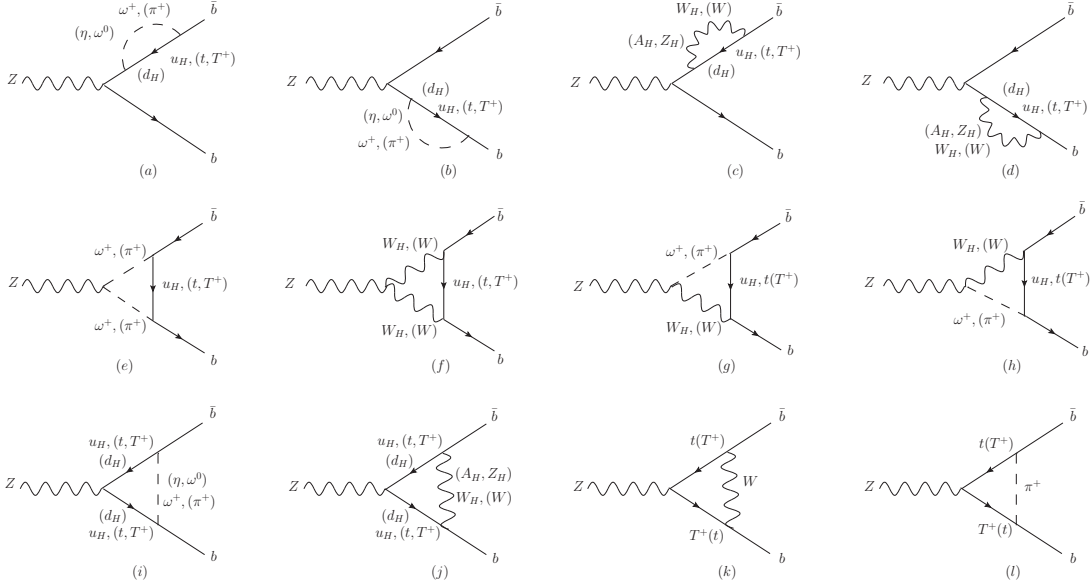


FIG. 1: Feynman diagrams of $Z \rightarrow b\bar{b}$ at one-loop level in the LHT model.

LOOPTOOLS [15]. The relevant Feynman rules can be found in Ref. [16]. We applied the on-shell renormalization scheme and have checked that the divergences are canceled.

In the numerical calculations we take the input parameters [17] as Fermi constant $G_F = 1.16637 \times 10^{-5} \text{GeV}^{-2}$, the fine-structure constant $\alpha = 1/128$, Z -boson mass $M_{Z_L} = 91.2 \text{GeV}$, fermion masses m_f , the electroweak mixing angle $S_W^2 = 0.231$ and the final-state asymmetry parameter $A_e = 0.1515$. In our calculation, the relevant LHT parameters are the scale f , the mixing parameter x_L , the mirror quark masses and parameters in the matrices V_{Hu} and V_{Hd} .

For the mirror quark masses, from Eq.(5) we get $m_{u_H^i} = m_{d_H^i}$ at $\mathcal{O}(v/f)$ and further assume

$$m_{u_H^1} = m_{u_H^2} = m_{d_H^1} = m_{d_H^2} = M_{12}, m_{u_H^3} = m_{d_H^3} = M_3 \quad (24)$$

For the matrices V_{Hu} and V_{Hd} , considering the constraints in Ref.[18], we study the completely generic scenario, i.e.the six parameters of V_{Hd} are arbitrary. After that, we follow Ref.[19] to consider the following two scenarios for comparison:

Scenario I: $V_{Hd} = 1, V_{Hu} = V_{CKM}^\dagger$

Scenario II: $S_{13}^d = 0.5, \delta_{12}^d = \delta_{23}^d = 0, \delta_{13}^d = \delta_{13}^{SM}, S_{ij}^d = S_{ij}^{SM}$ otherwise

Firstly, we discuss the R_b changes with the LHT parameters, the numerical results are

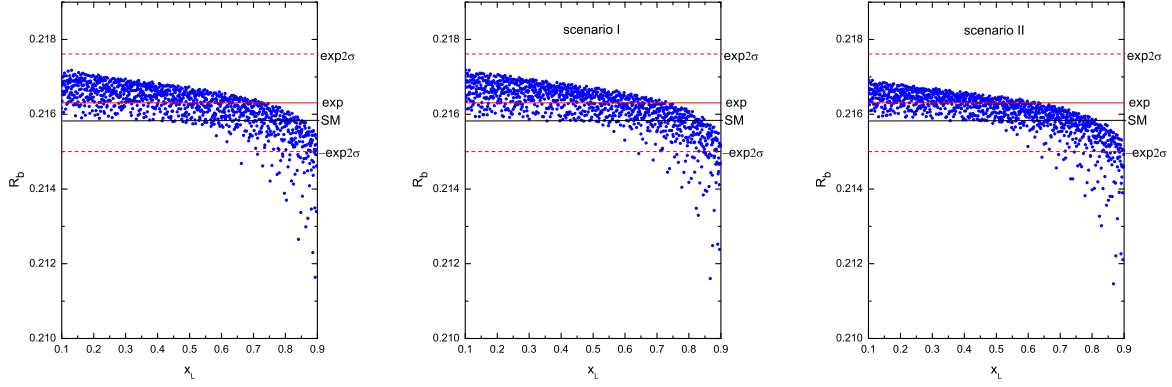


FIG. 2: Scatter plots of R_b versus x_L in arbitrary scenario, scenario I and scenario II, respectively. The experimental value $R_b = 0.21629 \pm 0.00066$.

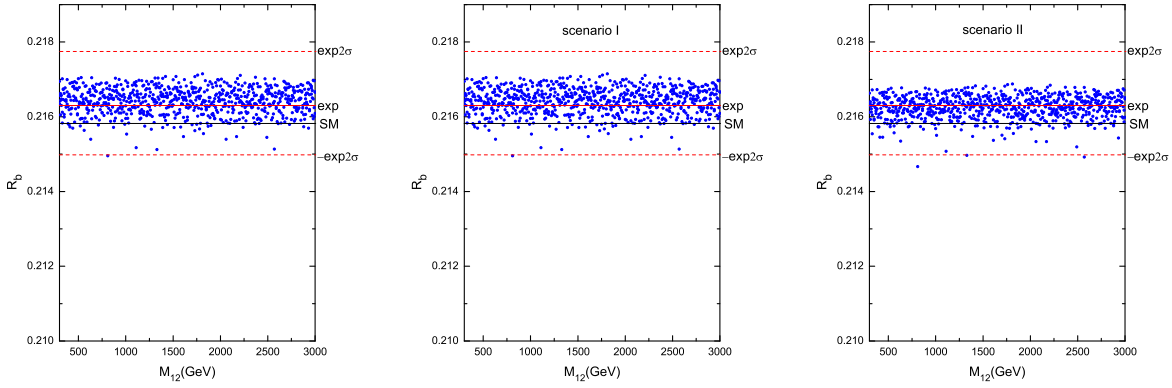


FIG. 3: Scatter plots of R_b versus M_{12} in three different scenarios, respectively. The experimental value $R_b = 0.21629 \pm 0.00066$.

summarized in Fig.(2-3). To see the influence of the mixing parameter x_L on the R_b , considering the existing constraints, we let the parameters vary randomly in the range: $M_{12} = 300 \sim 3000 \text{ GeV}$, $M_3 = 300 \sim 3000 \text{ GeV}$, $f = 400 \sim 3000 \text{ GeV}$. In these three scenarios, we can see the plots of R_b decline with the x_L increasing, which shows that the contribution of the mixing diagrams between t and T^+ is negative and becomes larger with the x_L increasing. When $x_L > 0.7$, part of the plots are beyond the 2σ regions of its experimental value. This feature is similar in three different scenarios.

To see the influence of the first two generation mirror quarks mass M_{12} on the R_b ,

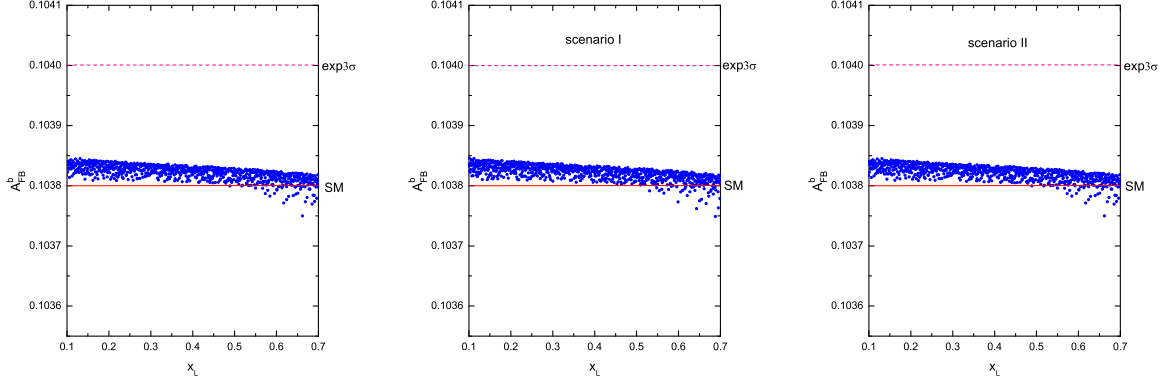


FIG. 4: Scatter plots of A_{FB}^b versus x_L in three different scenarios, respectively. The experimental value $A_{FB}^b = 0.0992 \pm 0.0016$.

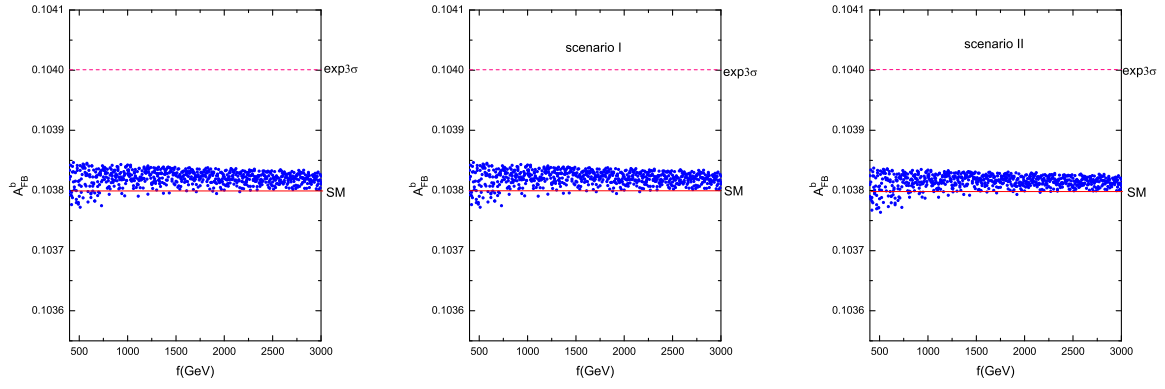


FIG. 5: Scatter plots of A_{FB}^b versus f in three different scenarios, respectively. The experimental value $A_{FB}^b = 0.0992 \pm 0.0016$.

considering the constraint from R_b on the x_L , we let the parameters vary randomly in the range: $M_3 = 300 \sim 3000 \text{ GeV}$, $f = 400 \sim 3000 \text{ GeV}$, $x_L = 0.1 \sim 0.7$. In these three scenarios, we can see the plots of R_b are almost in the 2σ regions of its experimental value. The noticeable feature is that the R_b isn't sensitive to M_{12} so that the constraint from R_b on M_{12} is very loose.

Secondly, we discuss the A_{FB}^b changes with the LHT parameters, the numerical results are summarized in Fig.(4-6). Same as the R_b , the A_{FB}^b isn't sensitive to M_{12} , so we don't give the figures of the A_{FB}^b as the function of M_{12} . To see the influence of the

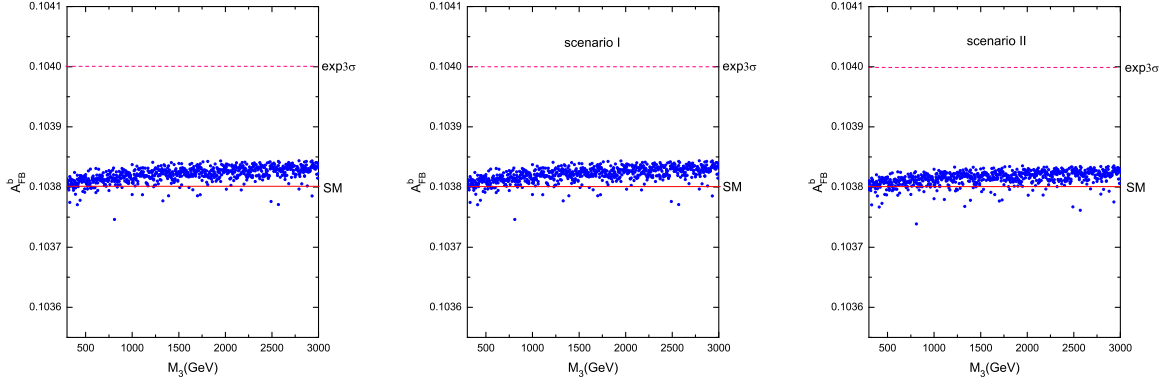


FIG. 6: Scatter plots of A_{FB}^b versus M_3 in three different scenarios, respectively. The experimental value $A_{FB}^b = 0.0992 \pm 0.0016$.

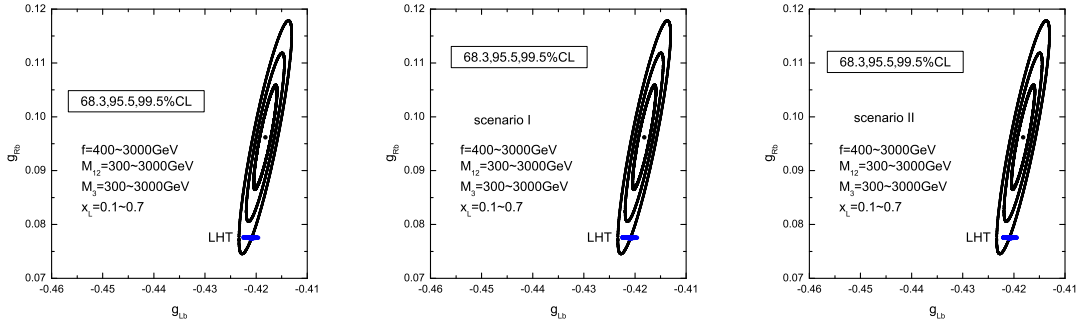


FIG. 7: The left-handed and right-handed coupling constants in the LHT model. The experimental value $g_L^b = -0.4182 \pm 0.0015$, $g_R^b = 0.0962 \pm 0.0063$.

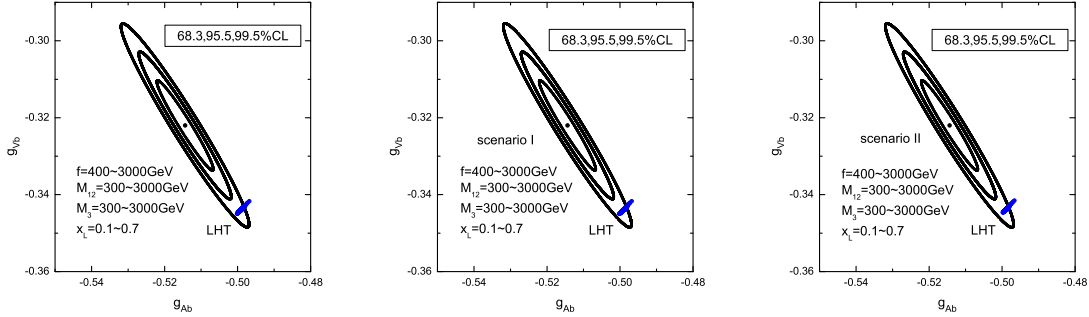


FIG. 8: The effective vector and axial-vector coupling constants in the LHT model. The experimental value $g_V^b = -0.3220 \pm 0.0077$, $g_A^b = -0.5144 \pm 0.0051$.

mixing parameter x_L on the A_{FB}^b , we let the parameters vary randomly in the range: $M_{12} = 300 \sim 3000 GeV$, $M_3 = 300 \sim 3000 GeV$, $f = 400 \sim 3000 GeV$. For the same reason, we can see the plots of A_{FB}^b decline and become closer to the experimental central value with the x_L increasing. However, the contribution of the new particles is not large enough so that the plots of the A_{FB}^b are still entirely scattered between the 2σ and 3σ region of its experimental value.

To see the influence of the scale f on the A_{FB}^b , we let the parameters vary randomly in the range: $M_{12} = 300 \sim 3000 GeV$, $M_3 = 300 \sim 3000 GeV$, $x_L = 0.1 \sim 0.7$. We can see the plots of A_{FB}^b are entirely between the 2σ and 3σ region of its experimental value. The plots of A_{FB}^b become closer to the SM with the f increasing, which shows that the contribution of the heavy particles decouples with the f increasing.

To see the influence of the third generation mirror quarks mass M_3 on the A_{FB}^b , we let the parameters vary randomly in the range: $M_{12} = 300 \sim 3000 GeV$, $f = 400 \sim 3000 GeV$, $x_L = 0.1 \sim 0.7$. We can see the plots of A_{FB}^b are entirely between the 2σ and 3σ region of its experimental value.

Finally, we discuss the Zbb couplings in the LHT model. In our calculation, we still consider the above three scenarios and let the parameters vary randomly in the range: $M_{12} = 300 \sim 3000 GeV$, $M_3 = 300 \sim 3000 GeV$, $f = 400 \sim 3000 GeV$, $x_L = 0.1 \sim 0.7$, the numerical results are summarized in Figs.(7-8). We confirm the result of Ref.[18], in which the correction from the mixing diagrams between t and T^+ to $Zb\bar{b}$ couplings is mainly on the g_L^b and doesn't have the correct sign to alleviate the large deviation between theoretical predictions and experimental values. The plots scatter beyond the 3σ region their experimental values are mainly caused by these couplings. Furthermore, the correction on the g_R^b is very small. However, there is a little difference when we consider the contributions involve other new particles. At this time, we can see part of the plots scatter in the 3σ internal region of their experimental values, where the deviation of g_L^b can be alleviated. Unfortunately, the correction on the g_R^b is still very small and the plots still scatter near the 3σ region of their experimental values so that the large deviation between theoretical predictions and experimental values can't be explained. The similar results are found on the g_A^b and g_V^b .

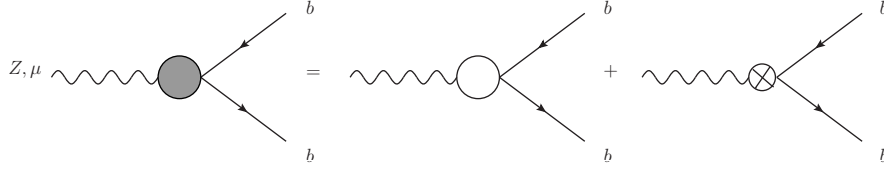
IV. CONCLUSIONS

In this paper, we studied the one-loop contributions of the new particles to the R_b and A_{FB}^b for three different scenarios in the framework of the LHT model. From the scatter plots of R_b versus x_L , the precision measurement data of R_b can give strong constraint on the x_L . Considering this constraint, we can see R_b isn't sensitive to the mass of the first two generation mirror quarks. The relevant parameters are weakly constrained by the precision measurement data of A_{FB}^b . In the given parameters space, the large deviation of A_{FB}^b can't be explained reasonably. From our study, the LHT model can provide the correction to the g_L^b and have small part of the parameter space to alleviate the deviation between theoretical predictions and experimental values. But the LHT model can't provide the large correction to the g_R^b so that the large deviation between the SM prediction predictions and experimental values of the Zbb couplings can't be alleviated substantially.

Acknowledgments

We would thank Junjie Cao and Lei Wu for useful discussions and providing the calculation programs. This work is supported by the National Natural Science Foundation of China under Grant Nos.10775039, 11075045, by Specialized Research Fund for the Doctoral Program of Higher Education under Grant No.20094104110001 and by HASTIT under Grant No.2009HASTIT004.

Appendix A: The expression of the renormalization vertex $\hat{\Gamma}_{Zb\bar{b}}^\mu$ [20]



$$\begin{aligned}\hat{\Gamma}_{Zb\bar{b}}^\mu &= \Gamma_{Zb\bar{b}}^\mu - ie\gamma^\mu(v_b - a_b\gamma_5)\frac{C_W}{2S_W}\delta Z_{ZA} - ieQ_b\gamma^\mu\frac{1}{2}\delta Z_{ZA} \\ &\quad + ie\gamma^\mu(v_b - a_b\gamma_5)\delta Z_V^b - ie\gamma^\mu\gamma_5(v_b - a_b\gamma_5)\delta Z_A^b\end{aligned}$$

where

$$\begin{aligned}v_b &\equiv \frac{I_b^3 - 2Q_b S_W^2}{2C_W S_W}, \quad a_b \equiv \frac{I_b^3}{2C_W S_W}, \quad I_b^3 = -\frac{1}{2}, \quad Q_b = -\frac{1}{3} \\ \delta Z_{ZA} &= 2\frac{\Sigma_T^{AZ}(0)}{M_{Z_L}^2} \\ \delta Z_L^b &= Re\Sigma_L^b(m_b^2) + m_b^2\frac{\partial}{\partial P_b^2}Re[\Sigma_L^b(P_b^2) + \Sigma_R^b(P_b^2) + 2\Sigma_S^b(P_b^2)]|_{P_b^2=m_b^2} \\ \delta Z_R^b &= Re\Sigma_R^b(m_b^2) + m_b^2\frac{\partial}{\partial P_b^2}Re[\Sigma_L^b(P_b^2) + \Sigma_R^b(P_b^2) + 2\Sigma_S^b(P_b^2)]|_{P_b^2=m_b^2} \\ \delta Z_V^b &= \frac{1}{2}(\delta Z_L^b + \delta Z_R^b), \delta Z_A^b = \frac{1}{2}(\delta Z_L^b - \delta Z_R^b)\end{aligned}$$

$$\begin{aligned}\hat{\Gamma}_{Zb\bar{b}}^{LHT,\mu} &= \Gamma_{Zb\bar{b}}^\mu(\pi^\pm) + \Gamma_{Zb\bar{b}}^\mu(\eta) + \Gamma_{Zb\bar{b}}^\mu(\omega^0) + \Gamma_{Zb\bar{b}}^\mu(\omega^\pm) + \Gamma_{Zb\bar{b}}^\mu(W_L^\pm) + \Gamma_{Zb\bar{b}}^\mu(A_H) + \Gamma_{Zb\bar{b}}^\mu(Z_H) \\ &\quad + \Gamma_{Zb\bar{b}}^\mu(W_H^\pm) + \Gamma_{Zb\bar{b}}^\mu(\pi^\pm, W_L^\pm) + \Gamma_{Zb\bar{b}}^\mu(\omega^\pm, W_H^\pm) + \delta\Gamma_{Zb\bar{b}}^\mu(\pi^\pm) + \delta\Gamma_{Zb\bar{b}}^\mu(\eta) + \delta\Gamma_{Zb\bar{b}}^\mu(\omega^0) \\ &\quad + \delta\Gamma_{Zb\bar{b}}^\mu(\omega^\pm) + \delta\Gamma_{Zb\bar{b}}^\mu(W_L^\pm) + \delta\Gamma_{Zb\bar{b}}^\mu(A_H) + \delta\Gamma_{Zb\bar{b}}^\mu(Z_H) + \delta\Gamma_{Zb\bar{b}}^\mu(W_H^\pm)\end{aligned}$$

Appendix B: The explicit expressions of the $\delta g_{L,R}^{LHT}$

They can be represented in form of 1-point, 2-point and 3-point standard functions A, B_0, B_1, C_{ij} . Here P_b and \bar{P}_b are outgoing. In all expressions, the mass of b-quark is ignored.

$$\begin{aligned}
\delta g_L = & \frac{1}{16\pi^2} g^2 C_W^2 (V_{Hd})_{i3}^* (V_{Hd})_{i3} m_{u_H}^2 C_0^a \\
& - \frac{1}{16\pi^2} \frac{g'^2}{100 M_{A_H}^2} (V_{Hd})_{i3}^* (V_{Hd})_{i3} \left\{ \left(-\frac{1}{2} + \frac{1}{3} S_W^2 \right) [m_{d_H}^4 C_0^b - m_{d_H}^2 M_{Z_L}^2 C_{12}^b - m_{d_H}^2 M_{Z_L}^2 C_{23}^b \right. \\
& - 2m_{d_H}^2 C_{24}^b + \frac{1}{2} m_{d_H}^2] - \frac{1}{2} \left[\frac{1}{2} m_{d_H}^2 B_0(-P_b, m_{d_H}^i, M_{A_H}) \right. \\
& + \frac{1}{2} m_{d_H}^2 (m_{d_H}^2 - M_{A_H}^2) \frac{\partial}{\partial P_b^2} B_0(-P_b, m_{d_H}^i, M_{A_H})] \\
& - \frac{1}{3} S_W^2 \left[-\frac{1}{2} m_{d_H}^2 B_0(-P_b, m_{d_H}^i, M_{A_H}) - \frac{1}{2} m_{d_H}^2 (m_{d_H}^2 - M_{A_H}^2) \frac{\partial}{\partial P_b^2} B_0(-P_b, m_{d_H}^i, M_{A_H}) \right] \Big\} \\
& - \frac{1}{16\pi^2} \frac{g^2}{4 M_{Z_H}^2} (V_{Hd})_{i3}^* (V_{Hd})_{i3} \left\{ \left(-\frac{1}{2} + \frac{1}{3} S_W^2 \right) [m_{d_H}^4 C_0^c - m_{d_H}^2 M_{Z_L}^2 C_{12}^c - m_{d_H}^2 M_{Z_L}^2 C_{23}^c \right. \\
& - 2m_{d_H}^2 C_{24}^c + \frac{1}{2} m_{d_H}^2] - \frac{1}{2} \left[\frac{1}{2} m_{d_H}^2 B_0(-P_b, m_{d_H}^i, M_{Z_H}) \right. \\
& + \frac{1}{2} m_{d_H}^2 (m_{d_H}^2 - M_{Z_H}^2) \frac{\partial}{\partial P_b^2} B_0(-P_b, m_{d_H}^i, M_{Z_H})] - \frac{1}{3} S_W^2 \left[-\frac{1}{2} m_{d_H}^2 B_0(-P_b, m_{d_H}^i, M_{Z_H}) \right. \\
& - \frac{1}{2} m_{d_H}^2 (m_{d_H}^2 - M_{Z_H}^2) \frac{\partial}{\partial P_b^2} B_0(-P_b, m_{d_H}^i, M_{Z_H})] \Big\} \\
& - \frac{1}{16\pi^2} \frac{g^2}{2 M_{W_H}^2} (V_{Hd})_{i3}^* (V_{Hd})_{i3} \left\{ \left(\frac{1}{2} - \frac{2}{3} S_W^2 \right) [m_{u_H}^4 C_0^d - m_{u_H}^2 M_{Z_L}^2 C_{12}^d - m_{u_H}^2 M_{Z_L}^2 C_{23}^d \right. \\
& - 2m_{u_H}^2 C_{24}^d + \frac{1}{2} m_{u_H}^2] - \frac{1}{2} \left[\frac{1}{2} m_{u_H}^2 B_0(-P_b, m_{u_H}^i, M_{W_H}) \right. \\
& + \frac{1}{2} m_{u_H}^2 (m_{u_H}^2 - M_{W_H}^2) \frac{\partial}{\partial P_b^2} B_0(-P_b, m_{u_H}^i, M_{W_H})] - \frac{1}{3} S_W^2 \left[-\frac{1}{2} m_{u_H}^2 B_0(-P_b, m_{u_H}^i, M_{W_H}) \right. \\
& - \frac{1}{2} m_{u_H}^2 (m_{u_H}^2 - M_{W_H}^2) \frac{\partial}{\partial P_b^2} B_0(-P_b, m_{u_H}^i, M_{W_H})] + 2C_W^2 m_{u_H}^2 C_{24}^e \Big\} \\
& - \frac{1}{16\pi^2} \frac{g'^2}{100} (V_{Hd})_{i3}^* (V_{Hd})_{i3} \left\{ \left(-\frac{1}{2} + \frac{1}{3} S_W^2 \right) [-2m_{d_H}^2 C_0^f + 2M_{Z_L}^2 C_{11}^f + 2M_{Z_L}^2 C_{23}^f \right. \\
& + 4C_{24}^f - 2] + \left[\frac{1}{2} B_0(-P_b, m_{d_H}^i, M_{A_H}) + \frac{1}{2} (m_{d_H}^2 - M_{A_H}^2) \frac{\partial}{\partial P_b^2} B_0(-P_b, m_{d_H}^i, M_{A_H}) \right. \\
& - \frac{1}{3} S_W^2 B_0(-P_b, m_{d_H}^i, M_{A_H}) - \frac{1}{3} S_W^2 (m_{d_H}^2 - M_{A_H}^2) \frac{\partial}{\partial P_b^2} B_0(-P_b, m_{d_H}^i, M_{A_H})] - \frac{1}{2} + \frac{1}{3} S_W^2 \Big\}
\end{aligned}$$

$$\begin{aligned}
& -\frac{1}{16\pi^2} \frac{g^2}{4} (V_{Hd})_{i3}^* (V_{Hd})_{i3} \left\{ \left(-\frac{1}{2} + \frac{1}{3} S_W^2\right) [-2m_{d_H}^2 C_0^g + 2M_{Z_L}^2 C_{11}^g + 2M_{Z_L}^2 C_{23}^g \right. \\
& + 4C_{24}^g - 2] + \left[\frac{1}{2} B_0(-P_b, m_{d_H}^i, M_{Z_H}) + \frac{1}{2} (m_{d_H}^2 - M_{Z_H}^2) \frac{\partial}{\partial P_b^2} B_0(-P_b, m_{d_H}^i, M_{Z_H}) \right. \\
& - \frac{1}{3} S_W^2 B_0(-P_b, m_{d_H}^i, M_{Z_H}) - \frac{1}{3} S_W^2 (m_{d_H}^2 - M_{Z_H}^2) \frac{\partial}{\partial P_b^2} B_0(-P_b, m_{d_H}^i, M_{Z_H})] - \frac{1}{2} + \frac{1}{3} S_W^2 \} \\
& + \frac{1}{16\pi^2} \frac{g^2}{2} (V_{Hd})_{i3}^* (V_{Hd})_{i3} \left(\frac{1}{2} - \frac{2}{3} S_W^2\right) [2m_{u_H}^2 C_0^h + 2M_{Z_L}^2 C_{11}^h + 2M_{Z_L}^2 C_{23}^h + 4C_{24}^h - 2] \\
& + \frac{1}{16\pi^2} \frac{g^2}{2} (V_{Hd})_{i3}^* (V_{Hd})_{i3} C_W^2 [-2M_{Z_L}^2 C_0^i - 2M_{Z_L}^2 C_{11}^i - 2M_{Z_L}^2 C_{23}^i - 12C_{24}^i + 2] \\
& + \frac{1}{16\pi^2} \frac{g^2}{2} (V_{Hd})_{i3}^* (V_{Hd})_{i3} \left[\frac{1}{2} B_0(-P_b, m_{u_H}^i, M_{W_H}) + \frac{1}{2} (m_{u_H}^2 - m_{W_H}^2) \frac{\partial}{\partial P_b^2} B_0(-P_b, m_{u_H}^i, M_{W_H}) \right. \\
& - \frac{1}{3} S_W^2 B_0(-P_b, m_{u_H}^i, M_{W_H}) - \frac{1}{3} S_W^2 (m_{u_H}^2 - M_{W_H}^2) \frac{\partial}{\partial P_b^2} B_0(-P_b, m_{u_H}^i, M_{W_H}) - \frac{1}{2} + \frac{1}{3} S_W^2] \\
& + \frac{1}{16\pi^2} \frac{g^2}{M_{Z_L}^2} C_W^2 [-2A(M_{W_H}) + 2M_{W_H}^2 B_0(0, M_{W_H}, M_{W_H}) + 2M_{W_H}^2 + M_{Z_L}^2 B_0(0, M_{W_H}, M_{W_H})] \\
& - \frac{1}{16\pi^2} \frac{2g^2}{M_{Z_L}^2} \left\{ \frac{2}{3} \left(\frac{1}{2} - \frac{2}{3} S_W^2\right) \left[-\frac{2}{3} A(m_{u_H}^i) + \frac{2}{3} m_{u_H}^2 B_0(0, m_{u_H}^i, m_{u_H}^i) + \frac{2}{3} m_{u_H}^2\right] \right. \\
& - \frac{1}{3} \left(-\frac{1}{2} + \frac{1}{3} S_W^2\right) \left[-\frac{2}{3} A(m_{d_H}^i) + \frac{2}{3} m_{d_H}^2 B_0(0, m_{d_H}^i, m_{d_H}^i) + \frac{2}{3} m_{d_H}^2\right] \\
& - \left(-\frac{1}{2} + S_W^2\right) \left[-\frac{2}{3} A(m_{l_H}^i) + \frac{2}{3} m_{l_H}^2 B_0(0, m_{l_H}^i, m_{l_H}^i) + \frac{2}{3} m_{l_H}^2\right] \} \\
& + \frac{g^2 x_L^2}{4M_{W_L}^2} (1 - 2S_W^2) \frac{v^2}{f^2} (V_{CKM})_{tb}^* (V_{CKM})_{tb} \frac{1}{16\pi^2} [-2m_{T^+}^2 + C_{24}^j] \\
& + \frac{g^2 x_L^2}{2M_{W_L}^2} \frac{v^2}{f^2} (V_{CKM})_{tb}^* (V_{CKM})_{tb} \frac{1}{16\pi^2} \left[\frac{2}{3} S_W^2 m_{T^+}^4 C_0^k - m_{T^+}^2 M_{Z_L}^2 C_{12}^k - \frac{2}{3} S_W^2 m_{T^+}^2 C_{23}^k \right. \\
& - \frac{4}{3} S_W^2 C_{24}^k + \frac{1}{3} S_W^2 m_{T^+}^2] \\
& + \frac{g^2 x_L^2}{4M_{W_L}^2} \frac{v^2}{f^2} (V_{CKM})_{tb}^* (V_{CKM})_{tb} \frac{1}{16\pi^2} \left\{ \frac{1}{2} m_{T^+}^2 B_0(-P_b, m_{T^+}, M_{W_L}) \right. \\
& + \frac{1}{2} m_{T^+}^2 (m_{T^+}^2 - M_{W_L}^2) \frac{\partial}{\partial P_b^2} B_0(-P_b, m_{T^+}, M_{W_L}) \\
& - \frac{1}{3} S_W^2 [m_{T^+}^2 B_0(-P_b, m_{T^+}, M_{W_L}) + m_{T^+}^2 (m_{T^+}^2 - M_{W_L}^2) \frac{\partial}{\partial P_b^2} B_0(-P_b, m_{T^+}, M_{W_L})] \} \\
& + \frac{g^2 x_L^2}{4M_{W_L}^2} \frac{v^2}{f^2} (V_{CKM})_{tb}^* (V_{CKM})_{tb} \frac{1}{16\pi^2} [-m_{T^+}^2 m_t^2 C_0^l] \\
& + \frac{g^2 x_L^2}{4M_{W_L}^2} \frac{v^2}{f^2} (V_{CKM})_{tb}^* (V_{CKM})_{tb} \frac{1}{16\pi^2} [-m_{T^+}^2 m_t^2 C_0^m] \\
& + \frac{g^2 x_L^2}{2} C_W^2 \frac{v^2}{f^2} (V_{CKM})_{tb}^* (V_{CKM})_{tb} \frac{1}{16\pi^2} [-2M_{Z_L}^2 C_0^j - 2M_{Z_L}^2 C_{11}^j - 2M_{Z_L}^2 C_{23}^j - 12C_{24}^j + 2] \\
& + \frac{g^2 x_L^2}{2} \frac{v^2}{f^2} (V_{CKM})_{tb}^* (V_{CKM})_{tb} \frac{1}{16\pi^2} \frac{2}{3} S_W^2 [m_{T^+}^2 C_0^k - 2M_{Z_L}^2 C_{11}^k - 2M_{Z_L}^2 C_{23}^k - \frac{4}{3} C_{24}^k + 2]
\end{aligned}$$

$$\begin{aligned}
& + \frac{g^2 x_L^2}{4} \frac{v^2}{f^2} (V_{CKM})_{tb}^* (V_{CKM})_{tb} \frac{1}{16\pi^2} [2M_{Z_L}^2 C_{11}^l + 2M_{Z_L}^2 C_{23}^l + 4C_{24}^l - 2] \\
& + \frac{g^2 x_L^2}{4} \frac{v^2}{f^2} (V_{CKM})_{tb}^* (V_{CKM})_{tb} \frac{1}{16\pi^2} [2M_{Z_L}^2 C_{11}^m + 2M_{Z_L}^2 C_{23}^m + 4C_{24}^m - 2] \\
& + \frac{g^2 x_L^2}{2} \frac{v^2}{f^2} (V_{CKM})_{tb}^* (V_{CKM})_{tb} \frac{1}{16\pi^2} [\frac{1}{2} B_0(-P_b, m_{T^+}, M_{W_L}) \\
& + (m_{T^+}^2 - M_{W_L}^2) \frac{\partial}{\partial P_b^2} B_0(-P_b, m_{T^+}, M_{W_L}) - \frac{1}{3} S_W^2 B_0(-P_b, m_{T^+}, M_{W_L}) \\
& - \frac{1}{3} S_W^2 (m_{T^+}^2 - M_{W_L}^2) \frac{\partial}{\partial P_b^2} B_0(-P_b, m_{T^+}, M_{W_L}) - \frac{1}{2} + \frac{1}{3} S_W^2] \\
& - \frac{g^2 x_L^2}{2} \frac{v^2}{f^2} (V_{CKM})_{tb}^* (V_{CKM})_{tb} \frac{1}{16\pi^2} [\frac{2}{3} S_W^2 m_{T^+}^2 C_0^n + 2(1 - \frac{2}{3} S_W^2) M_{Z_L}^2 C_{11}^n \\
& + 2(1 - \frac{2}{3} S_W^2) M_{Z_L}^2 C_{23}^n + 4(1 - \frac{2}{3} S_W^2) C_{24}^n - 2(1 - \frac{2}{3} S_W^2)] \\
& - \frac{g^2 x_L^2}{2} \frac{v^2}{f^2} (V_{CKM})_{tb}^* (V_{CKM})_{tb} \frac{1}{16\pi^2} [-2M_{Z_L}^2 C_0^o - 2M_{Z_L}^2 C_{11}^o - 2M_{Z_L}^2 C_{23}^o - 12C_{24}^o + 2] \\
& - \frac{g^2 x_L^2}{2} \frac{v^2}{f^2} (V_{CKM})_{tb}^* (V_{CKM})_{tb} \frac{1}{16\pi^2} [\frac{1}{2} B_0(-P_b, m_t, M_{W_L}) + \frac{1}{2} (m_t^2 - M_{W_L}^2) \frac{\partial}{\partial P_b^2} B_0(-P_b, m_t, M_{W_L}) \\
& - \frac{1}{3} S_W^2 B_0(-P_b, m_t, M_{W_L}) - \frac{1}{3} S_W^2 (m_t^2 - M_{W_L}^2) \frac{\partial}{\partial P_b^2} B_0(-P_b, m_t, M_{W_L}) - \frac{1}{2} + \frac{1}{3} S_W^2] \\
& - \frac{g^2 x_L^2}{2M_{W_L}^2} \frac{v^2}{f^2} (V_{CKM})_{tb}^* (V_{CKM})_{tb} \frac{1}{16\pi^2} [-m_t^4 (1 - \frac{2}{3} S_W^2) C_0^o - m_t^2 M_{Z_L}^2 C_{12}^o \\
& - \frac{2}{3} S_W^2 m_t^2 M_{Z_L}^2 C_{23}^o - \frac{4}{3} m_t^2 S_W^2 C_{24}^o(\bar{P}_b, P_b, m_t, M_{W_L}, m_t) + \frac{1}{3} S_W^2 m_t^2] \\
& - \frac{g^2 x_L^2}{4M_{W_L}^2} (1 - 2S_W^2) \frac{v^2}{f^2} (V_{CKM})_{tb}^* (V_{CKM})_{tb} \frac{1}{16\pi^2} [-2m_t^2 C_{24}^o] \\
& - \frac{g^2 x_L^2}{4M_{W_L}^2} \frac{v^2}{f^2} (V_{CKM})_{tb}^* (V_{CKM})_{tb} \frac{1}{16\pi^2} m_t^2 \{ \frac{1}{2} B_0(-P_b, m_t, M_{W_L}) \\
& + \frac{1}{2} (m_t^2 - M_{W_L}^2) \frac{\partial}{\partial P_b^2} B_0(-P_b, m_t, M_{W_L}) \\
& - \frac{1}{3} S_W^2 [B_0(-P_b, m_t, M_{W_L}) + (m_t^2 - M_{W_L}^2) \frac{\partial}{\partial P_b^2} B_0(-P_b, m_t, M_{W_L})] \} \\
& - \frac{g^2 x_L^2}{2} \frac{v^2}{f^2} S_W^2 (V_{CKM})_{tb}^* (V_{CKM})_{tb} \frac{1}{16\pi^2} [m_{T^+}^2 C_0^j(\bar{P}_b, P_b, M_{W_L}, m_{T^+}, M_{W_L})] \\
& - \frac{g^2 x_L^2}{2} \frac{v^2}{f^2} S_W^2 (V_{CKM})_{tb}^* (V_{CKM})_{tb} \frac{1}{16\pi^2} [m_{T^+}^2 C_0^j(\bar{P}_b, P_b, M_{W_L}, m_{T^+}, M_{W_L})] \\
& + \frac{g^2 x_L^2}{2} \frac{v^2}{f^2} S_W^2 (V_{CKM})_{tb}^* (V_{CKM})_{tb} \frac{1}{16\pi^2} [m_t^2 C_0^o(\bar{P}_b, P_b, M_{W_L}, m_t, M_{W_L})] \\
& + \frac{g^2 x_L^2}{2} \frac{v^2}{f^2} S_W^2 (V_{CKM})_{tb}^* (V_{CKM})_{tb} \frac{1}{16\pi^2} [m_t^2 C_0^o(\bar{P}_b, P_b, M_{W_L}, m_t, M_{W_L})]
\end{aligned}$$

$$\begin{aligned}
C_{ij}^a &= C_{ij}^a(\bar{P}_b, P_b, M_{W_H}, m_{u_H^i}, M_{W_H}) \\
C_{ij}^b &= C_{ij}^b(\bar{P}_b, P_b, m_{d_H^i}, M_{A_H}, m_{d_H^i}) \\
C_{ij}^c &= C_{ij}^c(\bar{P}_b, P_b, m_{d_H^i}, M_{Z_H}, m_{d_H^i}) \\
C_{ij}^d &= C_{ij}^d(\bar{P}_b, P_b, m_{u_H^i}, M_{W_H}, m_{u_H^i}) \\
C_{ij}^e &= C_{ij}^e(\bar{P}_b, P_b, M_{W_H}, m_{u_H^i}, M_{W_H}) \\
C_{ij}^f &= C_{ij}^f(\bar{P}_b, P_b, m_{d_H^i}, M_{A_H}, m_{d_H^i}) \\
C_{ij}^g &= C_{ij}^g(\bar{P}_b, P_b, m_{d_H^i}, M_{Z_H}, m_{d_H^i}) \\
C_{ij}^h &= C_{ij}^h(\bar{P}_b, P_b, m_{u_H^i}, M_{W_H}, m_{u_H^i}) \\
C_{ij}^i &= C_{ij}^i(\bar{P}_b, P_b, M_{W_H}, m_{u_H^i}, M_{W_H}) \\
C_{ij}^j &= C_{ij}^j(\bar{P}_b, P_b, M_{W_L}, m_{T^+}, M_{W_L}) \\
C_{ij}^k &= C_{ij}^k(\bar{P}_b, P_b, m_{T^+}, M_{W_L}, m_{T^+}) \\
C_{ij}^l &= C_{ij}^l(\bar{P}_b, P_b, m_t, M_{W_L}, m_{T^+}) \\
C_{ij}^m &= C_{ij}^m(\bar{P}_b, P_b, m_{T^+}, M_{W_L}, m_t) \\
C_{ij}^n &= C_{ij}^n(\bar{P}_b, P_b, m_t, M_{W_L}, m_t) \\
C_{ij}^o &= C_{ij}^o(\bar{P}_b, P_b, M_{W_L}, m_t, M_{W_L})
\end{aligned}$$

$$\begin{aligned}
\delta g_R = & -\frac{1}{16\pi^2} \frac{g'^2}{100M_{A_H}^2} (V_{Hd})_{i3}^* (V_{Hd})_{i3} \left\{ \frac{1}{3} S_W^2 m_{d_H^i}^2 B_1(-P_b, m_{d_H^i}, M_{A_H}) \right. \\
& - \frac{1}{3} S_W^2 \left[-\frac{1}{2} m_{d_H^i}^2 B_0(-P_b, m_{d_H^i}, M_{A_H}) - \frac{1}{2} m_{d_H^i}^2 (m_{d_H^i}^2 - M_{A_H}^2) \frac{\partial}{\partial P_b^2} B_0(-P_b, m_{d_H^i}, M_{A_H}) \right] \Big\} \\
& - \frac{1}{16\pi^2} \frac{g'^2}{4M_{Z_H}^2} (V_{Hd})_{i3}^* (V_{Hd})_{i3} \left\{ \frac{1}{3} S_W^2 m_{d_H^i} B_1(-P_b, m_{d_H^i}, M_{Z_H}) \right. \\
& - \frac{1}{3} S_W^2 \left[-\frac{1}{2} m_{d_H^i}^2 B_0(-P_b, m_{d_H^i}, M_{Z_H}) - \frac{1}{2} m_{d_H^i}^2 (m_{d_H^i}^2 - M_{Z_H}^2) \frac{\partial}{\partial P_b^2} B_0(-P_b, m_{d_H^i}, M_{Z_H}) \right] \Big\} \\
& + \frac{1}{16\pi^2} \frac{g'^2}{2M_{W_H}^2} (V_{Hd})_{i3}^* (V_{Hd})_{i3} \left\{ \frac{1}{3} S_W^2 m_{u_H^i} B_1(-P_b, m_{u_H^i}, M_{W_H}) \right. \\
& - \frac{1}{3} S_W^2 \left[-\frac{1}{2} m_{u_H^i}^2 B_0(-P_b, m_{u_H^i}, M_{W_H}) - \frac{1}{2} m_{u_H^i}^2 (m_{u_H^i}^2 - M_{W_H}^2) \frac{\partial}{\partial P_b^2} B_0(-P_b, m_{u_H^i}, M_{W_H}) \right] \Big\} \\
& - \frac{1}{16\pi^2} \frac{g'^2}{100} (V_{Hd})_{i3}^* (V_{Hd})_{i3} \left\{ \frac{2}{3} S_W^2 B_1(-P_b, m_{d_H^i}, M_{A_H}) + \frac{1}{3} S_W^2 B_0(-P_b, m_{d_H^i}, M_{A_H}) \right. \\
& + \frac{1}{3} S_W^2 (m_{d_H^i}^2 - M_{A_H}^2) \frac{\partial}{\partial P_b^2} B_0(-P_b, m_{d_H^i}, M_{A_H}) \Big\} \\
& - \frac{1}{16\pi^2} \frac{g'^2}{4} (V_{Hd})_{i3}^* (V_{Hd})_{i3} \left\{ \frac{2}{3} S_W^2 B_1(-P_b, m_{d_H^i}, M_{Z_H}) + \frac{1}{3} S_W^2 B_0(-P_b, m_{d_H^i}, M_{Z_H}) \right. \\
& + \frac{1}{3} S_W^2 (m_{d_H^i}^2 - M_{Z_H}^2) \frac{\partial}{\partial P_b^2} B_0(-P_b, m_{d_H^i}, M_{Z_H}) \Big\} \\
& - \frac{1}{16\pi^2} \frac{g'^2}{2} (V_{Hd})_{i3}^* (V_{Hd})_{i3} \left\{ \frac{2}{3} S_W^2 B_1(-P_b, m_{u_H^i}, M_{W_H}) + \frac{1}{3} S_W^2 B_0(-P_b, m_{u_H^i}, M_{W_H}) \right. \\
& + \frac{1}{3} S_W^2 (m_{u_H^i}^2 - M_{W_H}^2) \frac{\partial}{\partial P_b^2} B_0(-P_b, m_{u_H^i}, M_{W_H}) \Big\} \\
& + \frac{g^2 x_L^2}{4M_{W_L}^2} \frac{v^2}{f^2} (V_{CKM})_{tb}^* (V_{CKM})_{tb} \frac{1}{16\pi^2} \left\{ -\frac{2}{3} S_W^2 m_{T^+}^2 B_1(-P_b, m_{T^+}, M_{W_L}) \right. \\
& - \frac{2}{3} S_W^2 \left[\frac{1}{2} m_{T^+}^2 B_0(-P_b, m_{T^+}, M_{W_L}) + \frac{1}{2} m_{T^+}^2 (m_{T^+}^2 - M_{W_L}^2) \frac{\partial}{\partial P_b^2} B_0(-P_b, m_{T^+}, M_{W_L}) \right] \Big\} \\
& + \frac{g^2 x_L^2}{2} \frac{v^2}{f^2} (V_{CKM})_{tb}^* (V_{CKM})_{tb} \frac{1}{16\pi^2} \left\{ -\frac{2}{3} S_W^2 B_1(-P_b, m_{T^+}, M_{W_L}) \right. \\
& - \frac{1}{3} S_W^2 \left[B_0(-P_b, m_{T^+}, M_{W_L}) + (m_{T^+}^2 - M_{W_L}^2) \frac{\partial}{\partial P_b^2} B_0(-P_b, m_{T^+}, M_{W_L}) \right] \Big\} \\
& - \frac{g^2 x_L^2}{4M_{W_L}^2} \frac{v^2}{f^2} (V_{CKM})_{tb}^* (V_{CKM})_{tb} \frac{1}{16\pi^2} \left\{ -\frac{2}{3} S_W^2 m_t^2 B_1(-P_b, m_t, M_{W_L}) \right. \\
& - \frac{1}{3} S_W^2 \left[m_t^2 B_0(-P_b, m_t, M_{W_L}) + m_t^2 (m_t^2 - M_{W_L}^2) \frac{\partial}{\partial P_b^2} B_0(-P_b, m_t, M_{W_L}) \right] \Big\} \\
& - \frac{g^2 x_L^2}{2} \frac{v^2}{f^2} (V_{CKM})_{tb}^* (V_{CKM})_{tb} \frac{1}{16\pi^2} \left\{ -\frac{2}{3} S_W^2 B_1(-P_b, m_t, M_{W_L}) \right. \\
& - \frac{1}{3} S_W^2 \left[B_0(-P_b, m_t, M_{W_L}) + (m_t^2 - M_{W_L}^2) \frac{\partial}{\partial P_b^2} B_0(-P_b, m_t, M_{W_L}) \right] \Big\}
\end{aligned}$$

-
- [1] N. Arkani-Hamed, A. G. Cohen, and H. Georgi, Phys. Lett. B 513, 232 (2001); N. Arkani-Hamed, et al., JHEP 0208, 020 (2002); JHEP 0208, 021 (2002); I. Low, W. Skiba, and D. Smith, Phys. Rev. D 66, 072001 (2002); D. E. Kaplan and M. Schmaltz, JHEP 0310, 039(2003).
 - [2] N. Arkani-Hamed, A. G. Cohen, E. Katz, and A. E. Nelson, JHEP 0207, 034 (2002); S. Chang, JHEP 0312, 057 (2003); T. Han, H. E. Logan, B. McElrath, and L. T. Wang, Phys. Rev. D 67, 095004 (2003); M. Schmaltz and D. Tucker-smith, Ann. Rev. Nucl. Part. Sci. 55, 229 (2005).
 - [3] C. Csaki, J. Hubisz, G. D. Kribs, P. Meade, J. Terning, Phys. Rev. D 67, 115002 (2003); Phys. Rev. D 68, 035009 (2003); J. L. Hewett, F. J. Petriello, and T. G. Rizzo, JHEP 0310, 062 (2003); M. C. Chen and S. Dawson, Phys. Rev. D 70, 015003 (2004); M. C. Chen, et al., Mod. Phys. Lett. A 21, 621 (2006); W. Kilian and J. Reuter, Phys. Rev. D 70, 015004 (2004).
 - [4] G. Marandella, C. Schappacher and A. Strumia, Phys. Rev. D 72, 035014 (2005).
 - [5] H. C. Cheng and I. Low, JHEP 0309, 051 (2003); JHEP 0408, 061 (2004); I. Low, JHEP 0410, 067 (2004); J. Hubisz and P. Meade, Phys. Rev. D 71, 035016 (2005).
 - [6] D. Comelli and J. P. Silva, Phys. Rev. D 54(1996)1176; V. D. Barger, K. M. Cheung, P. Langaclar, Phys. Lett. B 381(1996)226; P. Bamert, C. P. Burgess, J. M. Cline, D. London, and E. Nardi, Phys. Rev. D 54(1996)4275; D. Atwood, L. Reina, and A. Soni, Phys. Rev. D 54(1996)3296.
 - [7] The ALEPH, CDF, D0, DELPHI, L3, OPAL, SLD Collaborations, the LEP Electroweak Working Group, the Tevatron Electroweak Working Group, and the SLD electroweak and heavy flavour groups, arXiv:0811.4682v1 [hep-ex] 28 Nov 2008.
 - [8] M. Blanke, et al., Phys. Lett. B 646, 253 (2007).
 - [9] V. A. Novikov, L. B. Okun, A. N. Rozanov, M. I. Vysotsky, Rept. Prog. Phys. 62, 1275-1332 (1999); Morris L. Swartz, Int. J. Mod. Phys. A 15S1 307-332 (2000).
 - [10] M. Boulware and D. Finnell, Phys. Rev. D 44, 2054 (1991); Junjie Cao, Zhaohua Xiong and Jin Min Yang, Phys. Rev. Lett. 88, 111802 (2002).

- [11] N.Gray,David J. Broadhurst, W. Grafe, K. Schilcher., Z.Phys. C48:673-680 (1990) 673;L.R. Surguladze,Phys.Lett. B341:60-72(1994).
- [12] M.E. Peskin and T. Takeuchi, Phys. Rev. D46,381(1992).
- [13] The ALEPH,DELPHI, L3, OPAL, SLD Collaborations,the LEP Electroweak Working Group,the SLD Electroweak and Heavy Flavour Groups,Phys.Rept.427:257(2006).
- [14] G. t Hooft and M. J. G. Veltman,Nucl. Phys. B 153, 365 (1979).
- [15] T. Hahn and M. Perez-Victoria, Computl. Phys. Commun. 118, 153 (1999); T. Hahn, Nucl. Phys. Proc. Suppl. 135, 333 (2004).
- [16] M.Blanke, et al., JHEP 0701:066 (2007).
- [17] C. Amsler, etal., Phys. Lett. B 667,1 (2008).
- [18] J.Hubisz, P.Meade, A.Noble, M.Perelstein,JHEP 0601:135(2006).
- [19] J.Hubisz, S. J. Lee, and G. Paz, JHEP 0606:041 (2006).
- [20] W.F.L.Hollik,Preprint,DESY 88-188(1988); A.Denner, Fortschr.Phys.41: 307-420 (1993).